Submitted to:
Review of Scientific Instrumentation

SRI'95 APS, Argonne National Lab
Argonne IL, October 18-20,1995

BNL-62394
CONF-9510119--9

Mammography Imaging Studies using a Laue Crystal Analyzer

RECEIVED
JAN 0 3 1995
OSTI

D. Chapman(1), W. Thomlinson(2), F. Arfelli(2,4), N. Gmür(2), Z. Zhong(2), R. Menk(2), R. E. Johnson(3), D. Washburn(3), E. Pisano(3), D. Sayers(5)

(1) CSRRI, Illinois Institute of Technology, 3301 S. Dearborn, Chicago, IL 60616 USA
(2) National Synchrotron Light Source, Brookhaven National Laboratory, Upton, NY 11973 USA
(3) University of North Carolina, Chapel Hill, NC 27599 USA
(4) INFN di Trieste and Università di Trieste, Trieste, Italy
(5) North Carolina State University, Raleigh, NC 27695 USA

Keywords: medical imaging, mammography

DISCLAIMER

This report was prepared as an account of work sponsored by an agency of the United States Government. Neither the United States Government nor any agency thereof, nor any of their employees, makes any warranty, express or implied, or assumes any legal liability or responsibility for the accuracy, completeness, or usefulness of any information, apparatus, product, or process disclosed, or represents that its use would not infringe privately owned rights. Reference herein to any specific commercial product, process, or service by trade name, trademark, manufacturer, or otherwise does not necessarily constitute or imply its endorsement, recommendation, or favoring by the United States Government or any agency thereof. The views and opinions of authors expressed herein do not necessarily state or reflect those of the United States Government or any agency thereof.

DISTRIBUTION OF THIS DOCUMENT IS UNLIMITED

*Work performed under the auspices of the U.S. Department of Energy, under contract DE-AC02-76CH00016

MASTER

Abstract

Synchrotron based mammography imaging experiments have been performed with monochromatic x-rays in which a laue crystal placed after the object being imaged has been used to split the beam transmitted through the object. The X27C R&D beamline at the National Synchrotron Light Source was used with the white beam monochromatized by a double crystal Si(111) monochromator tuned to 18keV. The imaging beam was a thin horizontal line approximately 0.5mm high by 100mm wide. Images were acquired in line scan mode with the phantom and detector both scanned together. The detector for these experiments was an image plate. A thin Si(111) laue analyzer was used to diffract a portion of the beam transmitted through the phantom before the image plate detector. This "scatter free" diffracted beam was then recorded on the image plate during the phantom scan. Since the thin laue crystal also transmitted a fraction of the incident beam, this beam was also simultaneously recorded on the image plate.

The imaging results are interpreted in terms of an x-ray schliere or refractive index inhomogeneities. The analyzer images taken at various points in the rocking curve will be presented.

Introduction

Synchrotron based mammography imaging experiments have been performed with monochromatic x-rays in which a laue crystal placed after the object being imaged has been used to split the beam transmitted through the object. The imaging beam was a thin horizontal line approximately 0.5mm high by 100mm wide. Images were acquired in line scan mode with the phantom and detector both scanned together. The detector for these experiments was an image plate. A thin Si(111) laue analyzer was used to diffract a portion of the beam transmitted through the phantom before the image plate detector. This "scatter free" diffracted beam was then recorded on the image plate during the phantom scan. Since the thin laue crystal also transmitted a fraction of the incident beam, this beam was also simultaneously recorded on the image plate.

The imaging results are interpreted in the context of schlieren optics in which refractive index inhomogeneities of a transparent media can be quantified and imaged. These techniques rely on an optical element which modulates the transmitted intensity according to a deviation angle of rays through a media. The crystal analyzer in the x-ray imaging system is the equivalent of such an element.

The X27C R&D beamline at the National Synchrotron Light Source was used for these experiments. This is a large general purpose white beam hutch. A double crystal bragg case monochromator was installed in the hutch to prepare a wide horizontal imaging beam at a photon energy of 16-25keV. An energy of 18keV was chosen for these experiments. This imaging beam was then monitored by an ionization chamber to

measure the skin entry dose to the various phantoms used to characterize the imaging system. Plastic absorbers were used to control the dose to the phantom. A fast shutter system was used to begin and end the exposure on the image plate. The shutter was opened when the scanning stage was at a constant velocity and was closed at the end of the scan range before the stage was slowed to a stop. The dose was controlled by a combination of incident beam plastic absorbers and the scanning speed. The phantom thickness was typically in the 4-8cm thickness range to simulate the attenuation of compressed breast tissue as would be the case in a conventional mammographic imaging procedure.

Exposures were made onto a 20x25cm image plate and were subsequently read on a Fuji BAS 2000 reader. Typical reading parameters were a sensitivity of 1000, a latitude of 4 and a resolution size of 100μm.

Imaging experiments were performed with and without a crystal analyzer. The arrangements are shown in figure 1. Only the experiments with the analyzer are presented here. Non-analyzer results will be discussed elsewhere[1]. The top arrangement in the figure is the non-analyzer setup while bottom shows the setup with the analyzer. The analyzer was place in the beam after it had passed throught the phantom. The crystal was set in the laue arrangement in which the beam is incident on one side of the crystal plate and the diffracted beam emerges from the other side and was set in the parallel crystal geometry with respect to the monochromator. The crystal was approximately one absorption length thick (μt=1.04, t=0.74 mm) at the 18 keV imaging energy and had an asymmetry angle of 26^0. This is thickness range referred to as the thin

crystal laue case in dynamical theory [2]. Figure 2 shows the theoretical and measured relative intensities from the crystal. Note the relatively large transmission directly through the crystal. The agreement between the calculation and measurement is quite good.

Since the crystal is semi-transparent, this feature allows two simultaneous exposures to be performed on the image plate. The separation between the analyzer and the image plate was set so that these two images could be recorded over the scanning range without overlap or spilling over the edges of the image plate. Thus two images were recorded in each scan; a 'direct' beam image and a diffracted beam image.

There are three regions of particular interest when using such an analyzer crystal to create images. Those regions are the left and right slopes of the diffracted beam rocking curve and the center peak position. As can be seen from the complex shape of the transmitted beam rocking curve, the low and high angle sides of the diffracted beam rocking curve are not equivalent for the transmitted beam. The half intensity point on the low angle side corresponds to a peak in the transmitted beam (the anomalous transmission side) while the half intensity point on the high angle side corresponds to a mimima in the transmission (anomalous absorption side)[2]. The peak of the diffracted beam corresponds to the high slope region of the transmission.

This behavior results in various imaging possibilities depending on the setting of the analyzer. Images were acquired (as much as the stablility of the analyzer would allow) at the following points in the diffracted beam rocking curve: at 1/2 peak intensity on the low and high angle side and at the peak.

These images for both the diffracted and transmitted beams are interpreted in the context of these rocking curves (ie. their intensity values and the dependence of the intensity vs angle).

ANALYSIS

The transmitted and diffracted beam images are a composite of two (sometimes competing) effects: absorption and refraction. The refractive part is based on calculating the very small angle deflections in the media due to thickness, density or material composition variations. The propagation of light through such an inhomogenous media is called "schliere". These angle deflections alter the intensity transmitted or diffracted by the analyzer according to the rocking curve. This is very similar to an optical system used to visualize and measure gradients in the refractive index, Töpler's schlieren method[3].

The optical schliere effect results when there is an effective gradient in the refractive index in a transparent media. The complication in the x-ray regime is that there will always be an attenuation of the beam as it traverses the object.

The gradient direction, in this case, is in the vertical direction or the projection of the diffraction vector onto the plane perpendicular to the transmitted beam. This direction is referred to as z. The beam path direction through the media is the x direction. Note that the imaging plane is the y-z plane. Assume that the media is composed of a single material with a varying refractive index and thickness, then the schlieren angle, δ, is:

$$\delta_z = \int_0^{t(y,z)} \frac{1}{n(x,y,z)} \frac{\partial n(x,y,z)}{\partial z} dx \qquad \text{Eqn. 1.}$$

The refractive index in the x-ray energy range is slightly less than one and is given approximately by[4]:

$$n(x,y,z) = 1 - \frac{r_0 \lambda^2 Z}{2\pi V}(x,y,z) \qquad \text{Eqn. 2.}$$

where r_0 is the classical electron radius (2.81×10^{-13} cm), λ is the x-ray wavelength and Z is the number of electronic charges in the volume V. The latter quantity, Z/V, depends on the spatial coordinates, x, y and z and is related to the material density, ρ, by $Z/V=(Z/A)\rho/m_{AMU}$, where A is the atomic number and m_{AMU} is the mass of a nucleon (1.66×10^{-24} g). Then the schlieren angle is approximately:

$$\delta_z \cong -\frac{r_0 \lambda^2}{2\pi m_{AMU}} \int_0^{t(y,z)} \frac{Z}{A}(x,y,z) \frac{\partial \rho(x,y,z)}{\partial z} dx \qquad \text{Eqn. 3.}$$

where the 1/n(x,y,z) term has been approximated by one to keep terms to first order in ρ. If equation 3 is simplified by assuming that the quantity Z/A is a constant and that all of the spatial dependence is in the density and thickness and that the gradient of density is constant with x, then the equation can be rewritten as:

$$\delta_z \cong -\frac{r_0 \lambda^2}{2\pi m_{AMU}} \frac{Z}{A} \frac{\partial \rho t(y,z)}{\partial z} \cong -(2.69 \times 10^{10}\, cm/g) \frac{Z}{A} \lambda^2 \frac{\partial \rho t(y,z)}{\partial z} \qquad \text{Eqn. 4.}$$

This equation gives the deviation angle of the transmitted beam through the object being imaged. In practice this angle is too small ($\delta \cong 10^{-6}$ radian) to result in spatially displaced beams in an image given the source size at the NSLS. Interference of the refracted beam with the direct beam would not be visible in this measurement[5]. The distance from the

phantom to image plate in our experiments is approximately 1m. This displacement is expected to be then ~10^{-5} m or ~10 μm. This angle is however sufficient to cause a intensity change with the analyzer in place. Angles in this range (10^{-6} radian, 1 μradian or 0.2 arc-seconds) can result in intensity variations of several percent (see the rocking curve in figure 2).

If the special case of a fixed density object with just thickness variations, a mean density of water (1 g/cm^3), an imaging energy of 18 keV and an effective Z/A of 0.5 is considered, then equation 4 can be further reduced to:

$$\delta_z \cong -(0.64\mu radians)\frac{\partial t(y,z)}{\partial z} \qquad \text{Eqn. 5}$$

This gives an indication of the scale of the deviation angles resulting from a thickness gradient.

The schlieren deflection angle results in a modulation of intensity since the reflectivity and transmissivity of the laue crystal is a function of the incident beam angle.

The intensity is also affected by the normal transmission through the object via:

$$\frac{I}{I_0} = \exp\left\{-\int_0^{t(y,z)} \frac{\mu}{\rho}(x,y,z)\rho(x,y,z)dx\right\} \cong \exp\left\{-\frac{\mu}{\rho}\rho t(y,z)\right\} \qquad \text{Eqn. 5.}$$

where μ/ρ is the massic absorption coefficient and ρ the mass density of the material. Therefore the image recorded on the image plate is proportional to:

$$\begin{bmatrix} I_R \\ I_T \end{bmatrix} \cong \exp\left\{-\frac{\mu}{\rho}\rho t(y,z)\right\}\begin{bmatrix} R(\theta_0+\delta_z) \\ T(\theta_0+\delta_z \end{bmatrix} \qquad \text{Eqn. 6.}$$

where I_R and I_T are the diffracted and transmitted beams onto the image plate respectively and the analyzer is set to θ_0 relative to the peak position and δ_Z is the schlieren angle.

Since the deviation angle, δ_Z, is presumed small the reflectivity and the transmissivity can be expanded as:

$$\begin{bmatrix} R(\theta_0+\delta_Z) \\ T(\theta_0+\delta_Z) \end{bmatrix} \cong \begin{bmatrix} R(\theta_0)+\frac{\partial R}{\partial \theta}\delta_Z \\ T(\theta_0)+\frac{\partial T}{\partial \theta}\delta_Z \end{bmatrix} \qquad \text{Eqn. 7.}$$

Substituting equation 7 into equation 6 gives:

$$\begin{bmatrix} I_R \\ I_T \end{bmatrix} \cong \exp\left\{-\frac{\mu}{\rho}\rho t(y,z)\right\}\left\{\begin{bmatrix} R(\theta_0) \\ T(\theta_0) \end{bmatrix} + \begin{bmatrix} \frac{\partial R(\theta_0)}{\partial \theta} \\ \frac{\partial T(\theta_0)}{\partial \theta} \end{bmatrix}\delta_z(y,z)\right\} \qquad \text{Eqn. 8.}$$

Thus there are two contributions to the intensity in the diffracted and transmitted beams through the analyzer crystal: 1) the "normal" transmission given by the absorption coefficient and modified by the transmissivity and reflectivity of the analyzer and 2) the schliere given by the product of the normal transmission, the slope of the reflectivity or transmissivity curve and the schlieren angle.

This equation can be easily solved for the absorption map, $\rho t(y,z)$, and the schlieren angle map, $\delta_z(y,z)$:

$$\rho t(y,z) = -\frac{1}{\frac{\mu}{\rho}}\ln\left\{\frac{I_T(y,z)\frac{\partial R}{\partial \theta}(\theta_0) - I_R(y,z)\frac{\partial T}{\partial \theta}(\theta_0)}{I_0\left[T(\theta_0)\frac{\partial R}{\partial \theta}(\theta_0) - R(\theta_0)\frac{\partial T}{\partial \theta}(\theta_0)\right]}\right\} \qquad \text{Eqn. 9.}$$

$$\delta_z(y,z) = \frac{I_R(y,z)T(\theta_0) - I_T R(\theta_0)}{I_T(y,z)\frac{\partial R}{\partial \theta}(\theta_0) - I_R(y,z)\frac{\partial T}{\partial \theta}(\theta_0)} \qquad \text{Eqn. 10.}$$

These equations will now be used to interpret images acquired with the laue analyzer.

RESULTS

The use of equations 9 and 10 require that the rocking curve angle, θ_0, at which the images were taken is known. This was determined by setting the analyzer angle to achieve the expected ionization chamber reading for the diffracted beam. This procedure could establish the region on the rocking curve, but, due to instrumental drifts occurring ine the time between the tuning of the analyzer and the acquisition of image data, could not be relied upon to give a precise rocking angle, θ_0. The best estimation of the rocking angle comes from the data from the image plate. There is generally a region of the image which is known to have no structure in the imaging beam. In this region, the schlieren angle must be zero. The rocking angle can be calculated using the reflected and transmitted intensities from the image. This procedure works very well and matched quite closely the desired analyzer setting.

To confirm the refractive index effects, images were acquired of a phantom which had known linear thickness variations, referred to as a "wedge" phantom. A full image of this phantom is shown in figure 3. The upper image is the diffracted beam image, I_R, and the bottom is the transmitted beam image, I_T. This full image was acquired at the peak of the diffracted beam, i.e. θ_0=0. The sensitivity to a refractive index gradient occurs along a line from the transmitted beam image to the diffracted beam image. A small region of the image was used to confirm a sensitivity to the gradient. This is a region with a Plexiglas sawtooth phantom. This phantom was composed of parallel Plexiglas prisms. These

prisms had a profile shown in figure 4 with a rising thickness gradient of $\tan(60^0)=1.73$ and a falling gradient of $\tan(30^0)=0.56$. The maximum height of the prisms are 1.14 mm with a repeat distance of 2.63mm. Figure 5 is a composite showing the diffracted and transmitted beam images as well as the resulting schlieren angle, δ_z, and thickness, ρt, images. These images are taken at three settings of the analyzer corresponding to the locations shown on the rocking curve. The far left set from the low angle side of the rocking curve at θ_0=-4.9 μradians, the middle set near the peak at θ_0=+1.5 μradians and the right set on the high angle side at θ_0=+10.7 μradians.

Averaged sections of each schlieren angle and thickness images were taken and plotted in figure 6 along with the expected theoretical values. The expected or theoretical values are based on the material parameters for Plexiglas ($\mu/\rho=0.69$ cm^2/g, $\rho=1.19$ g/cm^3) and the use of equation 5 for the refraction angle.

One noticebale feature in the image as well as the section line plot is that the image taken at the peak has little sensitivity to the gradient. This results from the use of equation 10 in a region where the reflectivity slope can change sign. A more complex equation should be used here or a self consistent solution using the rocking curve. The agreement becomes more tolerable away from the bragg peak. The best agreement between the measured and expected values occurs for the image taken at -4.9 μradians below the peak. At this position the measured $\Delta\rho t$ is approximately 25% below the expected value. The schlieren angle has the correct value for the low gradient sides of the prisms at approximately -0.5 μradians, however, on the high gradient side, the measured angle is approximately 34% below the expected value of 1.3μradians.

As was expected for the images taken at the bragg peak, there may be a failure of the equation to handle the relatively large deviation angles then there are large gradients in the index or material thickness.

CONCLUSION

Images of phantoms have been taken of phantoms using a laue crystal analyzer to create two images of the same object. Approximate equations have been derived to describe these images in terms of the analyzer rocking curve and the object being imaged. These two images can be combined to give an image of the absorption of the object (ρt image) and an image of the refractive index gradient or schlieren angle image (δ_z image). The analysis of these images in these terms look promising. There is satisfactory agreement between the measured and expected thicknesses and refraction angles.

Future measurements are planned to investigate the use of diffraction optics to enhance the features in mammographic imaging.

ACKNOWLEDGEMENTS

The authors would like to thank Dr. Jerry Hastings and Dr. D.P. Siddons for many useful discussions regarding the use of an analyzer crystal for imaging and Dr. Siddons for the beamtime on the X27C beamline without which these experiments would not have been possible. This work is supported by NIH R01 CA60193, the Dept. of Radiology, UNC and US DOE DE-AC02-76CH00016

REFERENCES

[1] N. Gmür , W. Thomlinson, R.E. Johnson, D. Washburn, E. Pisano, F. Arfelli, :L.D. Chapman, Z. Zhong, R. Menk, D. Sayers, A37, these proceedings.

[2] B.W. Batterman and H. Cole, Rev. Mod. Phys. **36**, 681 (1964).

[3]c.f. J.R. Meyer-Arendt, *Introduction to Classical and Modern Optics* (Prentice-Hall, Englewood Cliffs, New Jersey, 1972), Section 3.3, p. 315.

[4] R. W. James, *The Optical Principles of the Diffraction of X-Rays* (Ox Bow Press, Woodbridge, Connecticut 1982), Chapter 2, p. 54.

[5] C. Raven, A. Snigirev, I. Snigireva, P. Spanne, and A. Suvrov, A35, these proceedings.

Figure Captions

Figure 1. Schematic of Experimental Setup in the X27C hutch. a) shows the arrangement without the analyzer crystal, b) shows additions to the setup for imaging with laue crystal analyzer.

Figure 2. Measured and calculated laue crystal rocking curves. Measured rocking curve obtained with ionization chambers at the location of the image plate. Calculated curves based on a Si (111) laue crystal 0.7mm thick with an asymmetry angle of 26^0 at 18keV photon

Figure 3. Image of "wedge" phantom as read from image plate. Upper image is the diffracted beam image and the lower the transmitted beam image. Image was taken with the analyzer set at the diffraction peak.

Figure 4. Cross section view of the Plexiglas sawtooth phantom.

Figure 5. Composite figure showing a section of the sawtooth phantom acquired at various analyzer angle settings and the δ_z and ρt images derived from the measured diffracted, I_R, and transmitted, I_T, beam images. The quantities in the boxes are the reflectivity, transmissivity and their angular gradients required to transform the images. The left image set was taken at θ_0=–4.9μradians, the middle image at θ_0=+1.5μradians and θ_0=+10.7μradians.

Figure 5. Averaged line plots of a section of the sawtooth phantom image. The upper plot is the thickness image, $\Delta\rho t$, and the lower plot is the schlieren angle image, δ_z. The dotted line is the expected values based on the dimensions and composition of the

phantom. The solid line is the measured value from the data at θ_0=–4.9μradians, the dashed line at θ_0=+1.5μradians, and the dot-dash at θ_0=+10.7μradians.

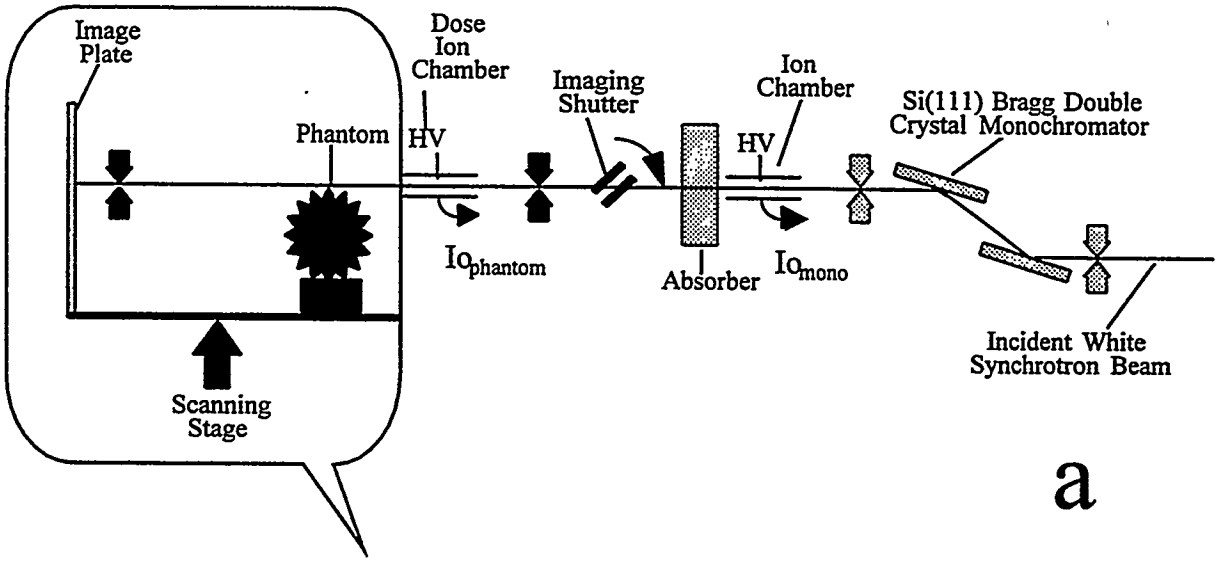
Image Plate
Dose Ion Chamber
Imaging Shutter
Ion Chamber
Si(111) Bragg Double Crystal Monochromator
Phantom
HV
HV
Io phantom
Absorber
Io mono
Incident White Synchrotron Beam
Scanning Stage

a

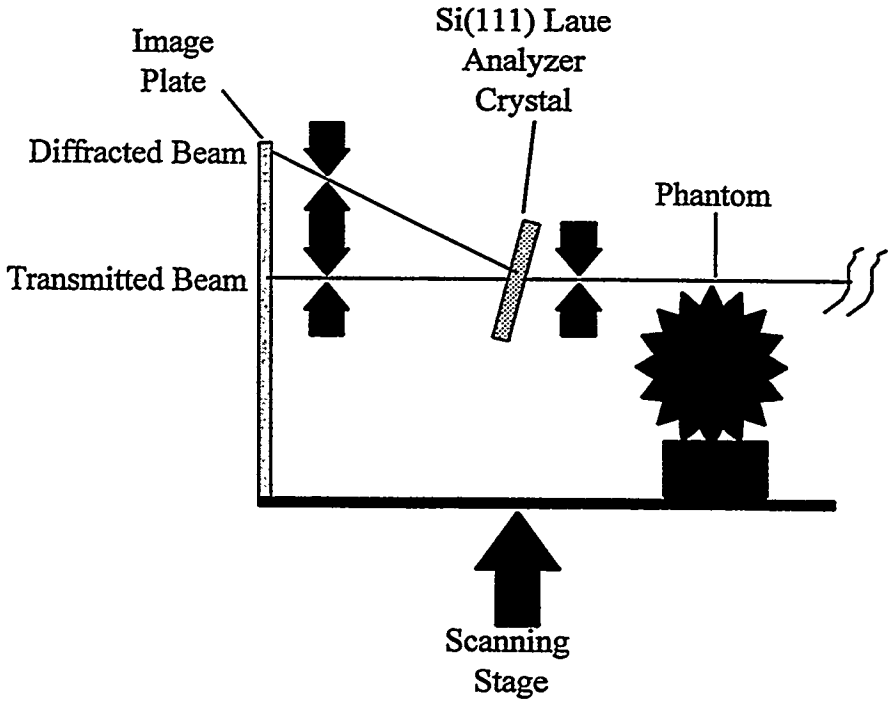
Image Plate
Si(111) Laue Analyzer Crystal
Diffracted Beam
Phantom
Transmitted Beam
Scanning Stage

b

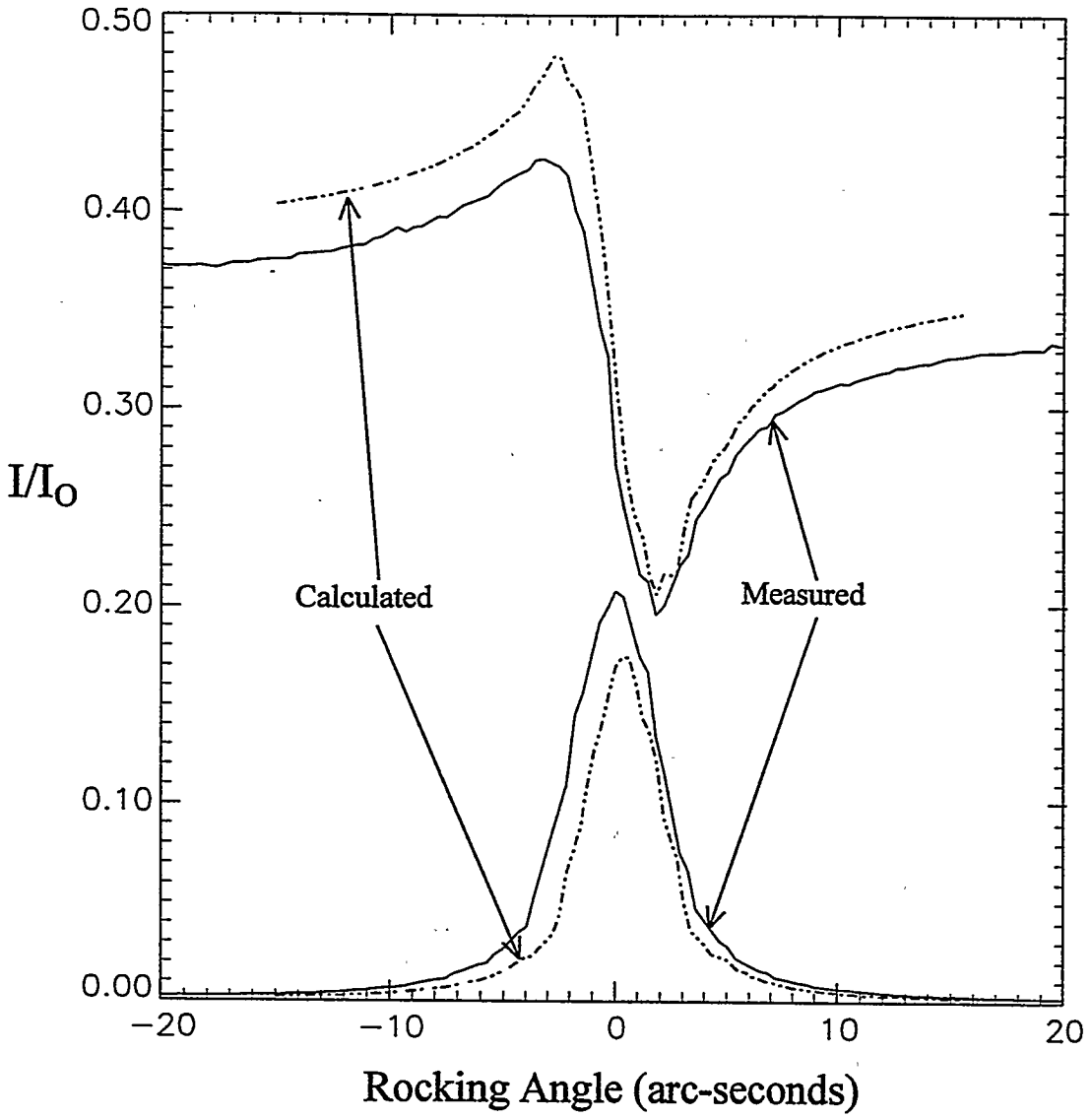
0.50
0.40
0.30
0.20
0.10
0.00
I/Io
Calculated
Measured
−20
−10
0
10
20
Rocking Angle (arc-seconds)

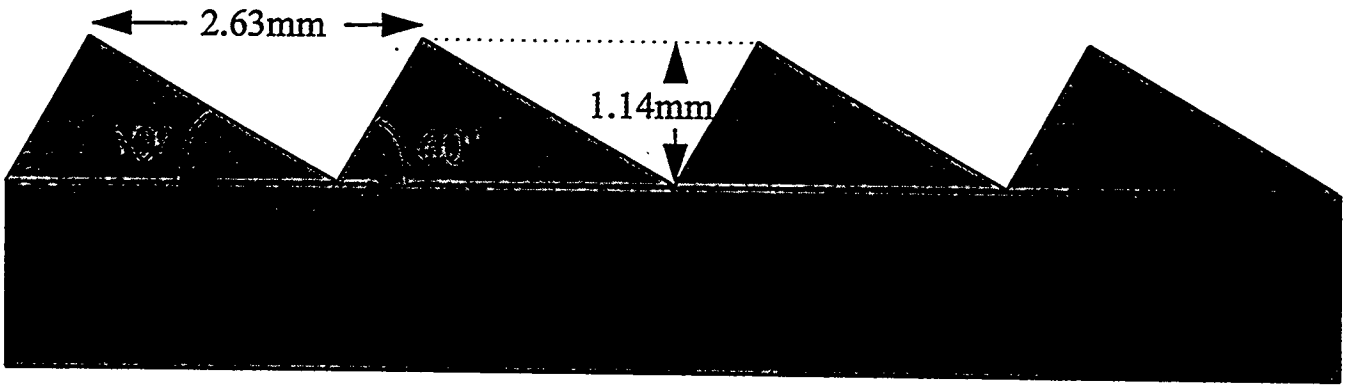
2.63mm
1.14mm

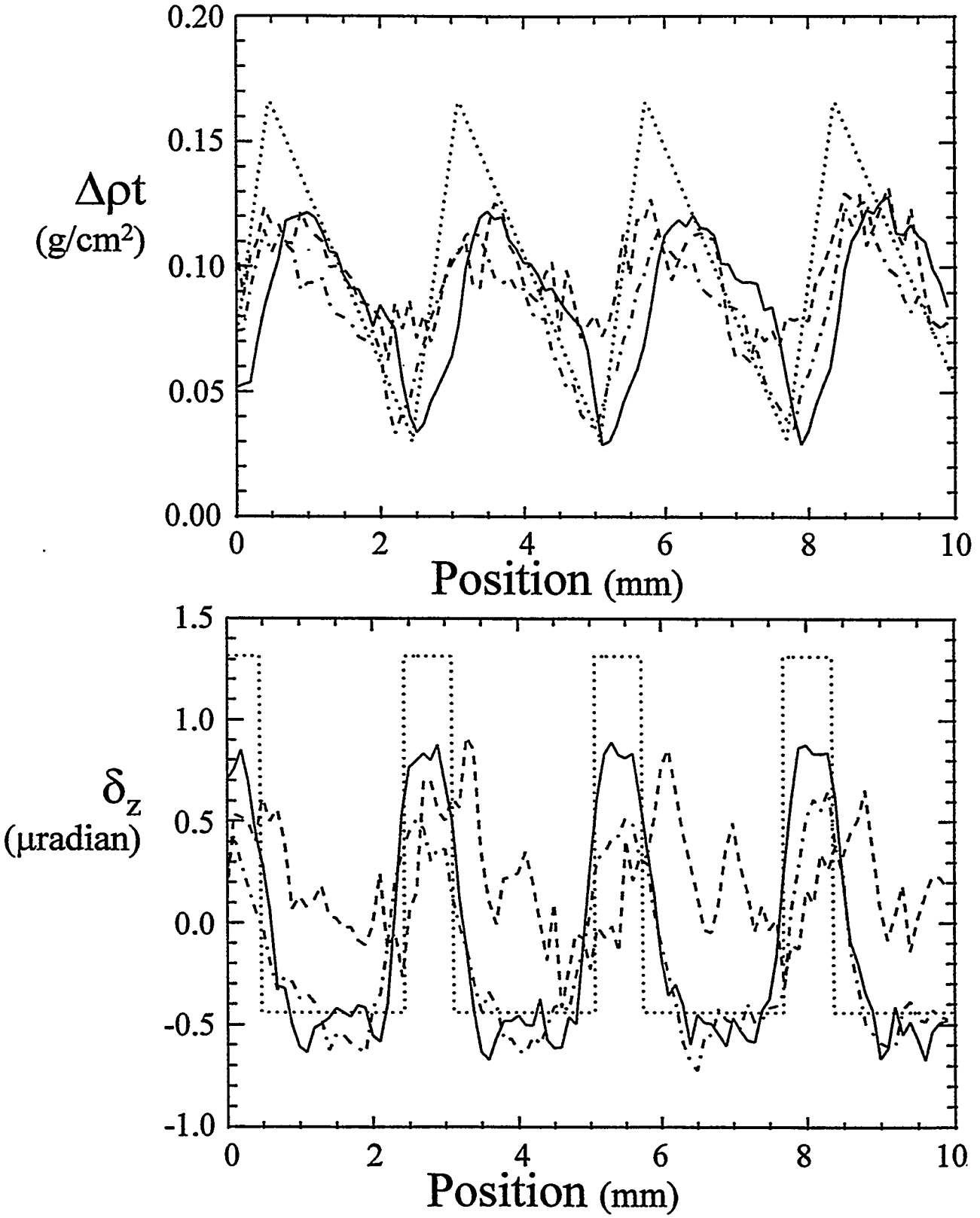
0.20
0.15
0.10
0.05
0.00
Δρt
(g/cm²)
0
2
4
6
8
10
Position (mm)
1.5
1.0
0.5
0.0
-0.5
-1.0
δz
(μradian)
0
2
4
6
8
10
Position (mm)